Fruit Defect Prediction Model (FDPM) based on Three-Level Validation

Yogesh[1] · Ashwani Kumar Dubey[1] · Rajeev Ratan Arora[2] · Ashish Mathur[3,4]

Abstract

It is a known fact that infrared radiation is produced by all objects with a temperature above absolute zero. In fruits, IR light sensor senses the invisible areas and exposes obscure objects in the image. In normal RGB images, it is very difficult to predict the internal defect of the fruit accurately without chopping it into pieces. In this paper, a thermal IR imaging-based fruit defect detection technique is proposed to identify and estimate the internal defect in the pome fruits. The technique is non-invasive and non-destructive which helps in minimizing the fruit wastage during the quality check. To achieve high accuracy, a three-level validation process is adopted. First level involves the prediction made by the proposed Deep learning-based expert system using RGB and thermal images of apple respectively. In second level, the validation of results is done using Fourier Transform Infrared spectroscopy technique. And finally, in third level, an invasive destructive method is used for inspection of the fruit quality by cutting them into pieces. The apple defect detection accuracy by the proposed Naïve Bayes classifier is observed to be 97.6% for thermal IR imaging samples whereas true color based achieved only 59% for the same sample. An apple seems to be healthy externally but internally there is a probability of a defect. Thermal IR imaging detects the heat from the surface of the fruit. Due to defective tissues of fruit pulp, the non-uniform temperature difference is observed and sensed on the surface of the fruit.

Keywords Apple quality · Deep learning · Fruit defect · FTIR · Pome fruit · Thermal image

✉ Ashwani Kumar Dubey
dubey1ak@gmail.com

Yogesh
eceyogesh@gmail.com

Rajeev Ratan Arora
rajeevratanarora@gmail.com

Ashish Mathur
nanoashish@gmail.com

1 Department of Electronics and Communication Engineering, Amity School of Engineering and Technology (ASET), Amity University Uttar Pradesh, Sector 125, Noida, UP 201313, India

2 Department of Electronics and Communication Engineering, MVN University, Aurangabad, Palwal, Haryana 121105, India

3 Department of Physics, School of Engineering, UPES University, Bidholi Campus, Dehradoon, India

4 Amity Institute of Nano Technology, Amity University Uttar Pradesh, Noida, UP 201313, India

1 Introduction

Fruit market growth counts on the high standard quality fruits. Generally, good quality fruits at low cost are the main concern for consumers. We observed that the fruits imported from other countries are of a high standard in terms of quality but too expensive as compared to the local market. The quality of the fruit is affected by the nutrients deficiency that causes defects in the fruits. Disorders in pome fruits may occur due to lack of Boron, Calcium, Nitrogen, Potassium, Magnesium, Phosphorous, and Zinc. The cause of the defect in pome fruits is due to nutrients deficiency, external impact, over-ripeness, bacterial effects, fungal effects, atmospheric conditions, storage type, packaging type, handling, and transportation, etc.

Few of the defects as stated above cannot be visualized externally. Hence, to visualize and estimate the internal defects in pome fruits, the property of thermal imaging is used, which works efficiently with good reliability and accuracy. It was observed that the defected regions represented by yellow and blue colors are due to unhealthy tissues, which causes non-uniform temperature distribution and on the

other hand, the healthy region denoted by red color reflects the uniform temperature distribution by the healthy tissues. This method minimizes the wastage of fruits and suggests the range of acceptance and rejections.

2 Relate Work

The heat inside the fruit causes enough temperature difference that is sensed on the surface of the fruit by thermal IR imaging technique. The defect in fruits is highlighted by the thermal imaging camera. Fourier transform near-infrared spectroscopy is used for the rapid estimation of starch, curcumin, and moisture contents in the sample for the online grading process [1]. The captured images are preprocessed before processing. The raw image is properly processed to have an accurate setup, especially in the hot spot detection system. The thermal image is accurately justified for abnormalities detection for faulty tracing by applying the Discrete Wavelet Transform (DWT) in thermal infrared image processing. The thermal image may tend to have noise made up of an uncertain entity during image capturing [2]. The thermal wave imaging method permits the depth scanning of the object. It is suitable for sub-surface defect detection [3]. For analyzing internal defects, the thermal image acquisition technique used, and its color pallets are utilized to detect anomalies. Frameworks for saliency which detect the salient object, hence improve performance substantially that is closely relative to hierarchical segmentation [4]. Mostly, a segmentation model has three aspects such as shape similarity, shape matching, and graph matching [5, 6]. Optimal threshold-based image segmentation increases accuracy and speed [7]. Timely identification of nutrient deficiencies aids in avert yield loss [8]. Artificial intelligence is used for efficient prediction [9]. In an improved thresholding segmentation approach, which is based on the maximum variance algorithm, at first Sobel operator is used to extract grayscale information and then the Otsu method is applied to extracted grayscale information for locating desirable segmentation level [10, 11]. Speeded-up robust feature (SURF) descriptor and artificial neural network (ANN) classifier are widely being used in feature extraction algorithms and classification algorithms respectively [12–14]. Supervised texture-based segmentation and recognition techniques are also being used in computer visions. The convolutional neural network identifies the infected region using deep learning [15, 16]. The problems of over and under segmentation need to be removed before the further processing of the region of interest [17, 18].

As far as segmentation of thermographic images is concerned, most of the methods were proposed or applied either in medical image thermography to segment the malignant tissues [19–22], or in electrical monitoring systems to identify the hotspots [23, 24] but none of the methods were reported to identify the healthy and defected portions from the thermal images of pome fruits. Hence, to fulfill this gap, we have developed a method to identify the defected and healthy portions of the pome fruits using thermal imaging. The thermal imaging is a non-destructive and non-invasive technique; hence, the chance of fruit wastage during quality check is reduced to be a minimum acceptable level.

3 Fruit Defect Prediction Model (FDPM)

In the proposed model, a deep learning-based expert system is developed which can analyze and detect the type of defect and deficiency in the fruit. The Block diagram of the proposed FDPM model is presented in Fig. 1.

3.1 Thermal Imaging of Fruit Sample

Thermal images are usually grayscale where black objects represent the cold region and white objects represent the hot region, the depth of gray shows the variation between the two [25, 26]. The thermal camera captures the infrared radiation from the objects [27, 28]. To help the user to identify objects at a different temperature, color is added to the images [29, 30] such as red, orange, green, purple, yellow, and blue [29]. Conventionally red color represents a source of heat and blue color represents an insignificant heat source [29–31].

During the quality inspection of fruit based on RGB imaging, it always remains challenging that the fruit looks good externally may also be good internally. The depth of penetration varied between 0 and 7 mm. The maximum depth for Jonagold apples observed to be 5.5 mm. Jeroen et al. measured wavelength in the range of 480–800 nm. The depth of penetration observed wavelength dependent:
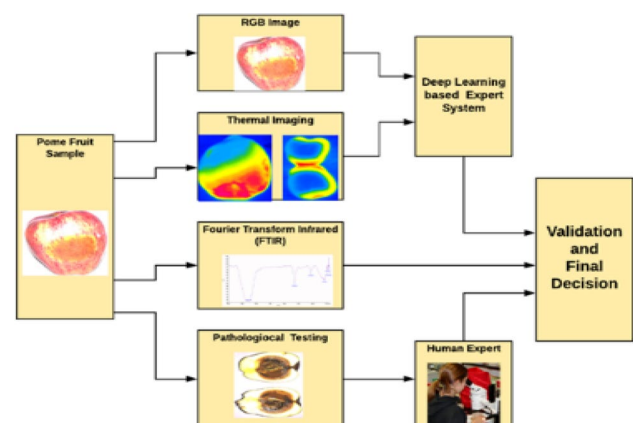

Fig. 1 Block diagram of the proposed Fruit Defect Prediction Model (FDPM)

up to 4 mm in the 700–900 nm range and between 2 and 3 mm in the 900–1900 nm range. A factor of 1.96 i.e. 95% pseudo-interval provides higher penetration depths of NIR radiation into fruit tissue [32]. Hence, the use of thermal imaging reduces this limitation by detecting the temperature difference inside the fruit and sense on the surface of the fruit. The automatic surface defect detection of fruit is possible by advances in the computer vision technique. The thermal images are captured at the temperature of 26 °C. The intensity of the light source is kept high enough to penetrate through the apple skin and gather information about the apple parenchyma tissue [32–36]. The computer vision-based fruit defect detection technique detects the peripheral defected region of fruit [37] whereas the thermal images [38, 39] detects internal as well as the external defect of the fruit.

In the proposed method, more than 500 thermal and 800 RGB image samples of apple are captured at the same temperature from an equal distance. The dimensions of the images are kept 227×227 pixels and saved in PNG format for lossless compression. Figure 2 shows a set of thermal images of apple samples having some internal disorders. In this, the red color represents the hot region and the blue color represents the cold region.

3.2 Deep Learning Algorithm for FDPM

Figure 3 illustrates the flow chart of the deep learning algorithm of the proposed FDPM that includes input image, convolution, pooling, linear rectified (ReLu), fully connected network, softmax, and output. The features of the input image are extracted by the convolution layer. It preserves the correlation between pixels by learning image features. The convolution layer is a mathematical operation that takes two inputs such as an image matrix and a filter. The filters perform the dot products with the input of the previous convolution layers as we proceed deeper. It takes the smaller colored pieces or edges and provides the larger pieces out of them. The feature map values are calculated using [40] as shown in (1):
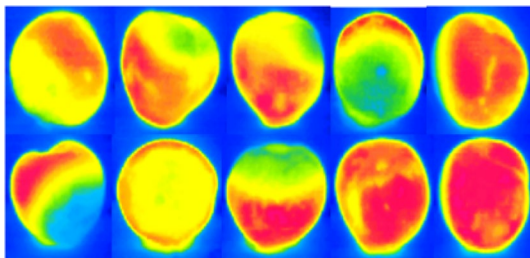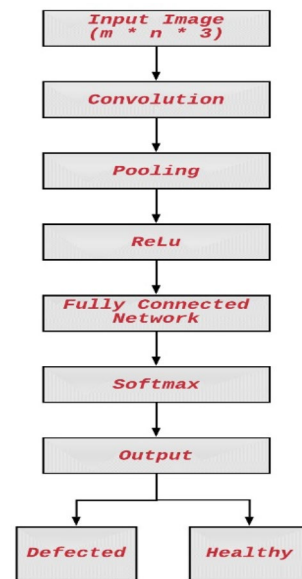

Fig. 2 Thermal images of apple sample

Fig. 3 Deep learning algorithm for FDPM

$$F[m, n] = (i * f)[m, n] = \sum_p \sum_q f[p, q] i[m - p, n - q] \quad (1)$$

where, 'i' and 'f' represent the input image and filter respectively. (m × n) shows the dimension of the resultant matrix. The spatial size of the representation is reduced by applying a pooling layer that results in the minimization of the parameters and computation in the network. It operates independently on each feature map. In this paper, max pooling is applied that summarizes the most activated presence of a feature in the network.

The activation function (rectified linear unit) is applied as defined in [40] and shown in (2):

$$y = \max(0, x) \quad (2)$$

The value of function 'y' is linear for all values greater than zero and zero for all negative values. The next layer is a fully connected layer that holds the composite and arrogates information from all the convolution layers. Each convolution layer holds the local features that include edges, shapes, corners, etc. The fully connected layer represents the feature vector for the input that is used for the classification of the defected apple after training of the network. This feature vector is also used during training to determine the loss and aid the network to get trained. To determine the predicted output classes as defected or healthy, softmax is used that map the non-linear output to a probability distribution over predicted output classes. Based on these predictions, the output is classified as defected or not. If the probability value lies between 0 to 0.5 then it is considered a healthy apple and for values greater than 0.5 is considered a defected apple. Mathematically it is defined in (3):

$if (p < 0.5), output = \}Healthy$'

$if (p \geq 0.5), output = \}Defected$' (3)

where 'p' represents the probability distribution over predicted output classes.
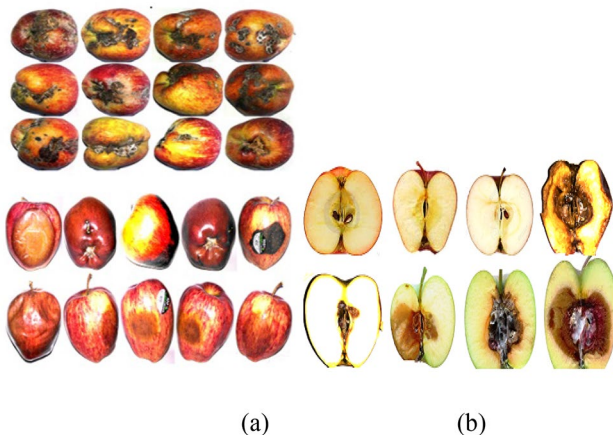

(a)   (b)

Fig. 4 **a** External appearance (RGB images) of apple samples having some defects. **b** Internal defects in apple samples

3.3 Validation Process of FDPM

A prediction about the defects in the given sample is made by the proposed FDPM (Fig. 3) based on the external appearance (i.e. RGB image) Fig. 4a, its internal defects in apple samples Fig. 4b, and internal images of apple (i.e. thermal image) of apple as shown in Fig. 5. In the thermal image, it is observed that the segmented reddish region represents the healthy region and the bluish region represents the defected region of the apple.

The histograms of the thermal image of a few samples are shown in Figs. 6, 7, 8, 9, 10, and 11 to visualize the intensity distribution for better prediction.

To validate the results, apple samples are taken randomly as shown in Fig. 5 in which the external appearance of apple in RGB and their correspondent thermal images along with the internal appearance in RGB with their correlated thermal images are considered. The proposed model identifies the defected portion of apple more precisely as compared to other conventional methods [41]. The internal disorder is clearly identified which is not possible manually or through an RGB image that was taken without cutting the fruit. Traditional methods applied for internal defect detection uses chemicals, bio-chemicals or NIR spectroscopy NMR, acoustic resonance, and MRI [42, 43]. But these techniques are unhygienic and costlier approach for internal defect detection of fruits as compared to the proposed FDPM. This paper primarily focuses on internal defects or disorder detection without touching or cutting the fruit.

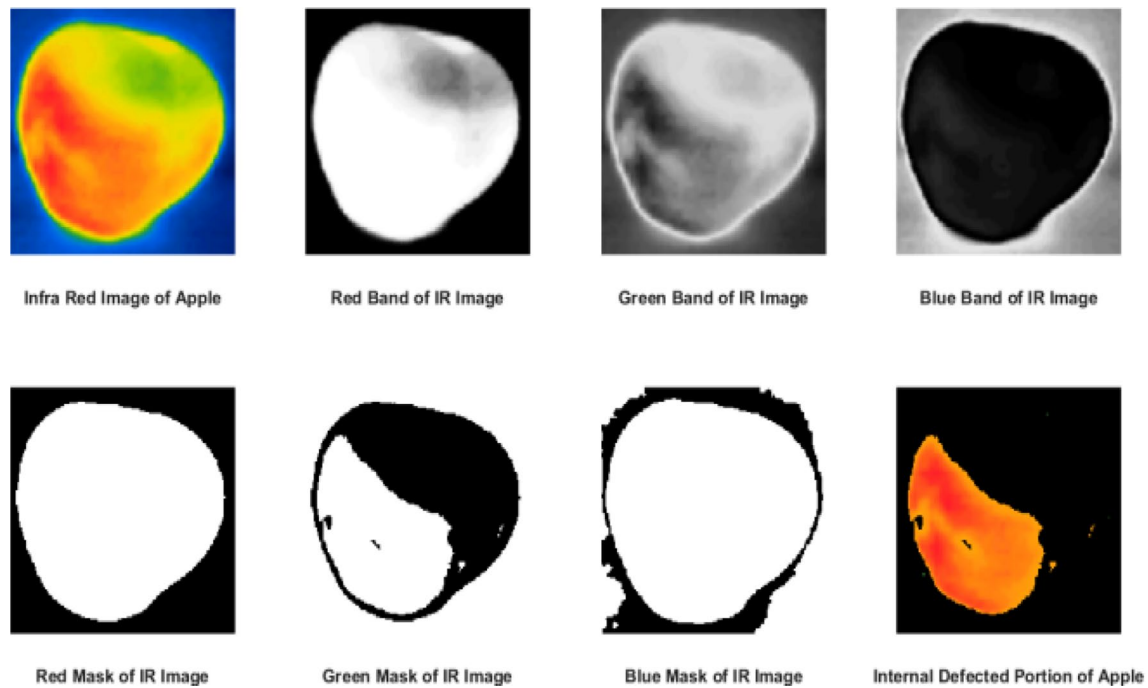**Fig. 5** External and internal appearance of thermal and RGB image of apple samples
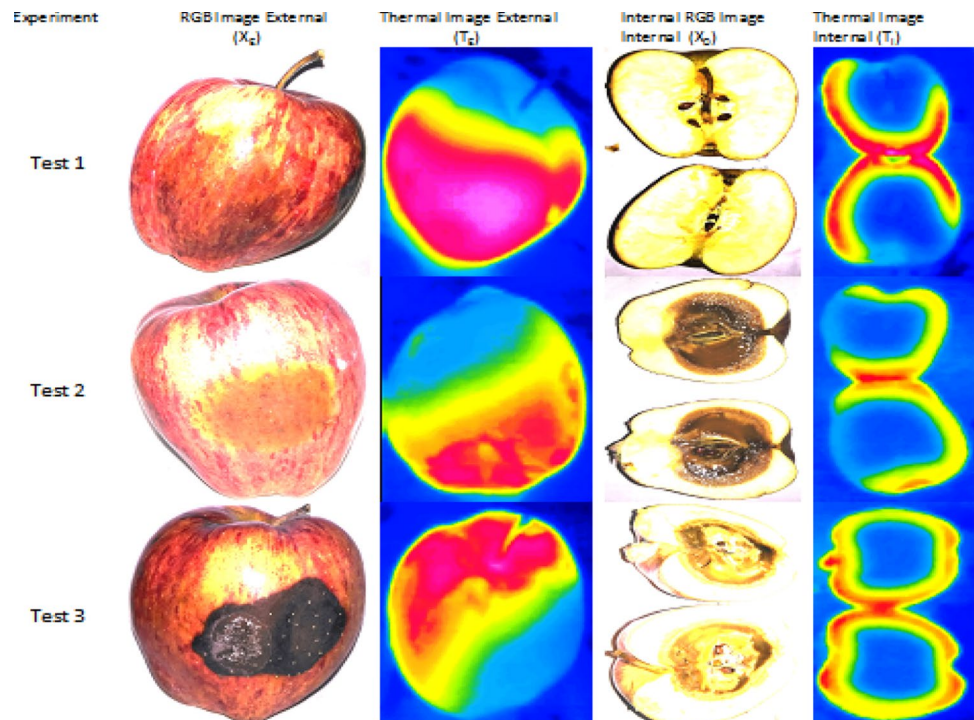
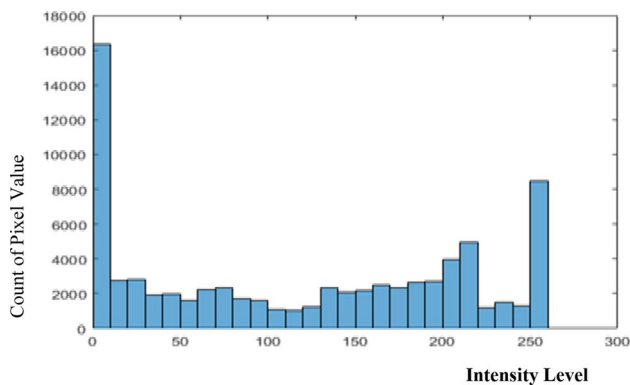**Fig. 6** Segmentation of healthy region of apple from sample 1

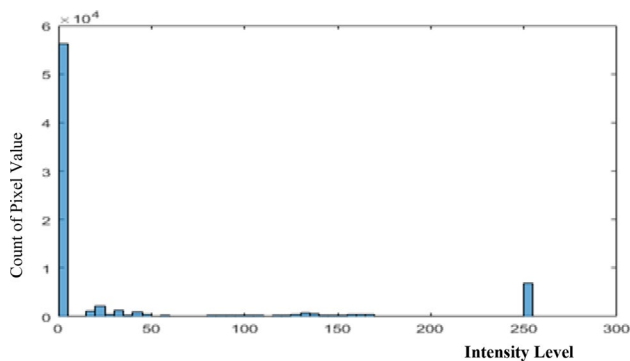

Fig. 7 Histogram of thermal image of sample 1

Fig. 8 Histogram of segmented image of sample 1

The extracted features retrieved from image contents like color, texture, and shape, which are difficult to find using traditional methods, are used for further analysis. A color thresholding-based segmentation technique as described by [44] is applied on the thermal images having different color pallets to segment out the region of interest i.e. defected and healthy portions of apples which cannot be seen through the external structure of the image. Thermal imaging improves the visibility of the object by detecting the object's infrared radiation and creating an electronic image that is based on that information. The Stefan-Boltzmann law finds the relationship between the object temperature and the amount of radiation that it emits. The radiation penetrates the apple tissue and reflects the radiation due to internal scattering that needs to be separated from that due to specular reflection. The camera detects the reflected temperature. The reflected temperature is nothing but the thermal radiation originating from other objects that reflect off the target that is being measured [32]. The emissivity measures heat at the surface of an object that is described in the range of 0.01 to 0.99 on the emissivity scale. The defected region is segmented by the hierarchical clustering method (Fuzzy C-Means algorithm) [44].

Few more apple samples having disorders due to nutrients deficiency are shown in Fig. 12. Hence, computer vision-based fruit recognition is relatively challenging due to the selection of suitable classifier for irregular features such as texture, contour, intensity, and size [45]. The irregularity in
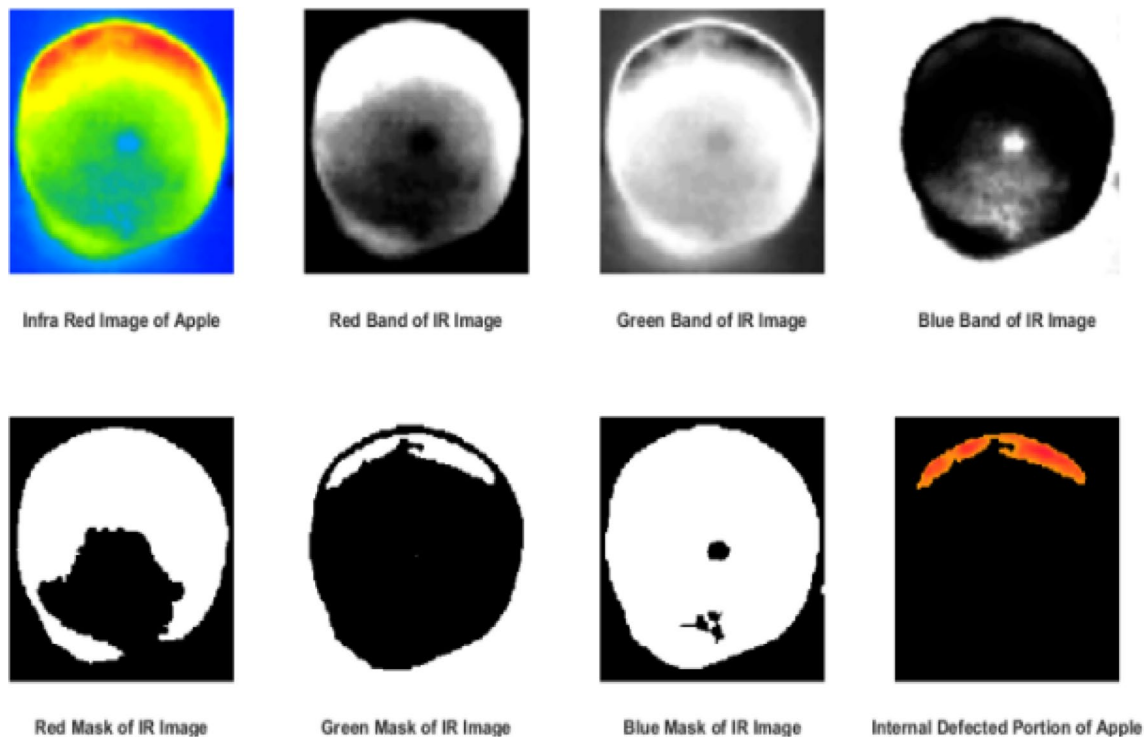
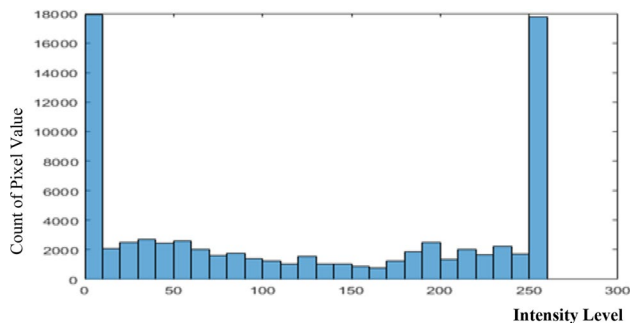**Fig. 9** Segmentation of healthy region of apple sample 2
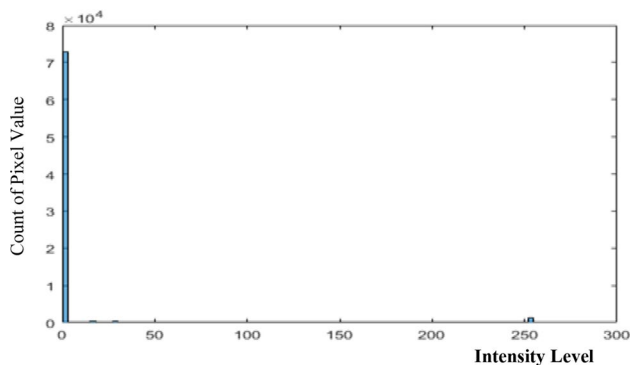

Fig. 10 Histogram of thermal image of sample 2

Fig. 11 Histogram of segmented image of sample 2

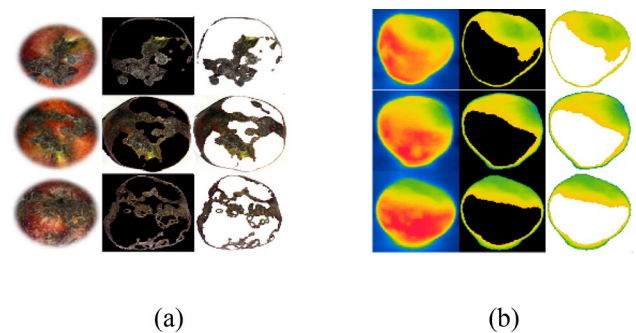

(a)   (b)

Fig. 12 a RGB Imaging defected region segmentation of apple, **b** Thermal Imaging defected region segmentation of apple
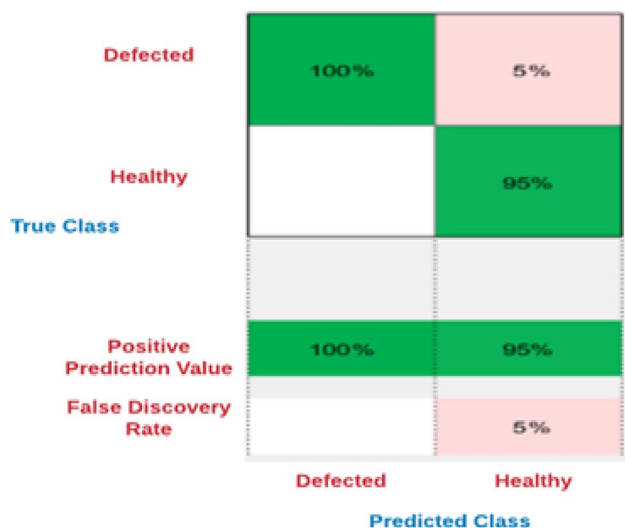
features may be due to bacterial effect, fungal effect, nutrient deficiency, physical impact, soil condition, and environmental condition.

3.4 Fourier Transform Infrared (FTIR) Spectroscopy of Fruit Samples

Further, second stage validation with Fourier Transform Infrared (FTIR) spectroscopy analyzes the healthy and defected apples by representing various functional groups. In comparison, functional group mismatch in healthy and defected apple is observed that distinguish the healthy and defected fruit. The FTIR spectroscopy method applied is

Table 1 Geometrical parameters of fruit samples

Sample no	Area	Centroid	Eccentricity	Solidity	Diameter	Convex area
Set 1	5828	68.667	0.79094	0.86623	86.142	6728
Set 2	5510	52.606	0.82796	0.84212	83.759	6543
Set 3	3553	94.168	0.89063	0.89025	67.259	3991
Set 4	13,809	84.51	0.41692	0.96546	132.6	14,303
Set 5	11,550	86.326	0.56919	0.83436	121.27	13,843
Set 6	5649	78.321	0.87218	0.87324	84.809	6469
Set 7	771	66.218	0.88666	0.076992	31.332	10,014
Set 8	3116	49.66	0.91818	0.80579	62.987	3867
Set 9	9371	84.742	0.43427	0.92062	109.23	10,179
Set 10	1314	79.454	0.97571	0.44377	40.903	2961

Fig. 13 Confusion matrix of the predicted model

Fig. 14 FTIR Analysis of defected sample: [Web source: http://all-craft.missouri.edu/carbon_romanos_2012/]

based on a destructive approach. It provides the molecular level changes in healthy and deficient samples.

In this research paper, three level sample validation is done. First is based on the true color and a thermal imaging-based approach, the second is the FTIR spectroscopy-based approach and the last one is the destructive approach.

4 Results and Discussions

The geometrical features of a few fruit samples are represented in Table 1, having the unit of pixel. These features are utilized for training and validation of the classifier model. The confusion matrix of a two-class classifier of fruit is shown in Fig. 13. The true positive (TP) is observed to be 100% as it predicts defected i.e. positive in predicted class and it's true in the actual class. It predicts true negative (TN) to be 5% as the predicted class predicts healthy and it's true.

False-positive (FP) is found to be 0%. False-negative (FN) is 95%.

The results are validated for the same set of samples using FTIR analysis and the destructive approach. From FTIR analysis, healthy apples having more absorption levels compared to defected apples as shown in Fig. 14. In healthy apples, the maximum absorption level in the functional group is at 3365.85 cm^{-1} as shown in Fig. 15, whereas in defected apples it is observed at 3332 and 3266.81 as shown in Figs. 16 and 17. Through the change in functional groups and fingerprints in FTIR analysis graph condition of fruit is determined whether it is healthy or defected. A comparative FTIR analysis of apple is shown in Fig. 18.

Further, this method can be extended to check the ripeness percentage of the fruits, internal disorder due to chemical effect, and to check the nutrients deficiency of fruits. The method may help the farmers and horticulturists to standardize their processes for better production and quality. In Fig. 19, the bin represents the number of vertical bars on the graph. The error range is divided into 20 bins. The vertical bar represents the number of samples from datasets. In a regression plot, it is observed that there is no outlier

Fig. 15 FTIR of healthy apple
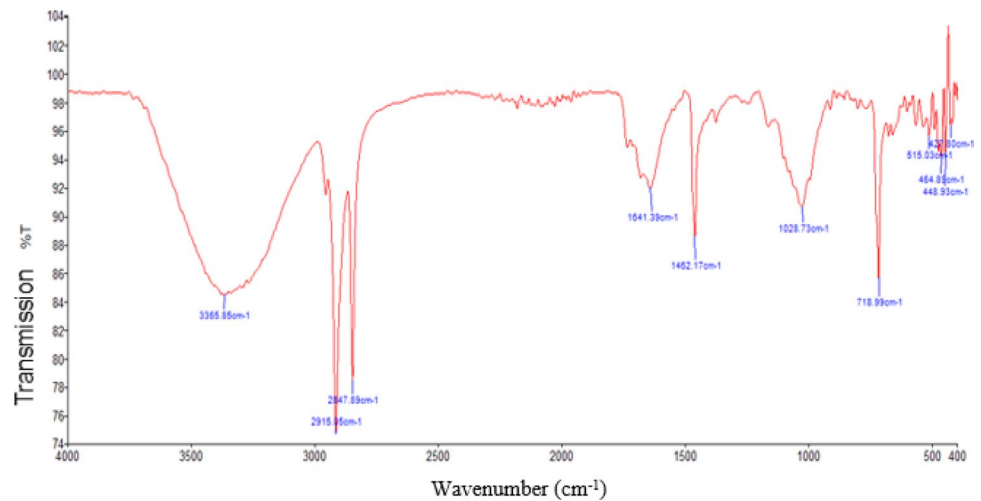
Fig. 16 FTIR of defected apple sample1
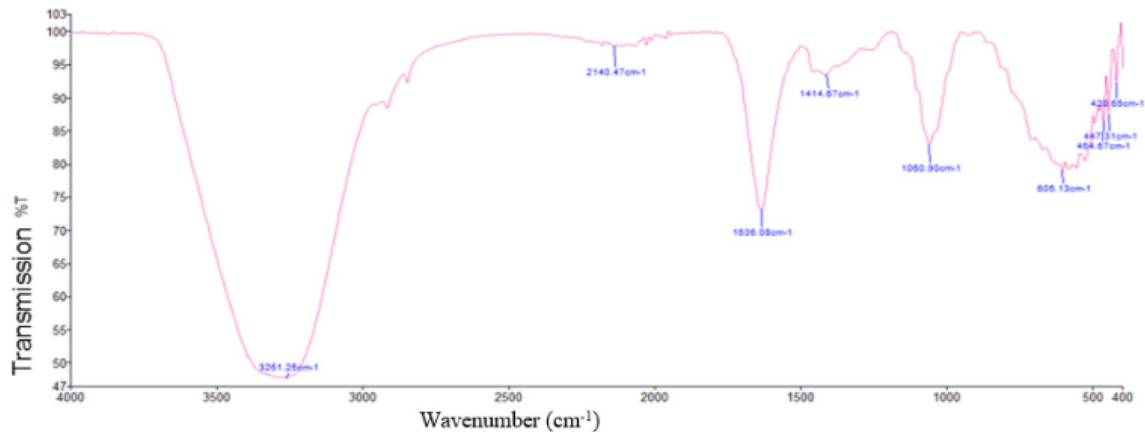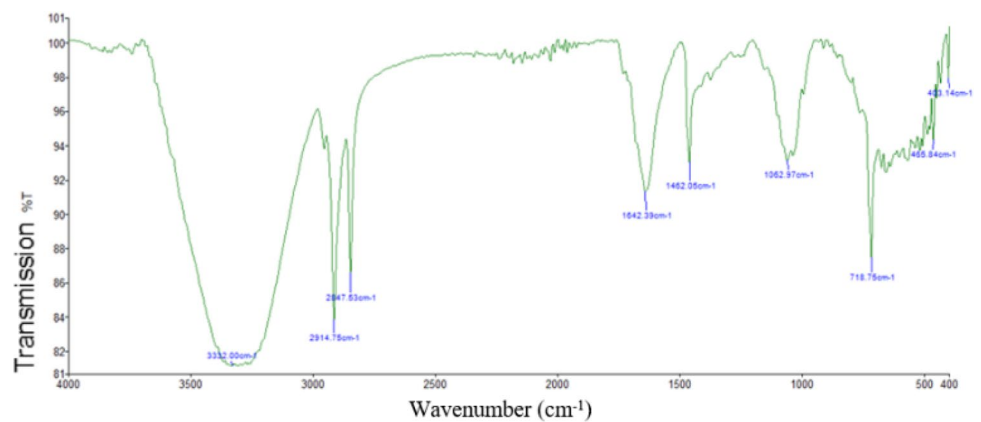
Fig. 17 FTIR of defected apple sample2

as shown in Fig. 20, hence, it indicates no erroneous data. Table 2 represents the performance comparison of different classification methods for fruit defects prediction. In this, the Naïve Bayes classifier detects and recognizes the defected apple with an accuracy of 97.6% for thermal IR imaging but the same sample with true color achieves only 59% accuracy. The huge difference in accuracy is due to infrared rays that can penetrate the apple and senses the invisible areas and exposes obscure objects in the sample. But the true color has the limitation and are unable to penetrate. As IR

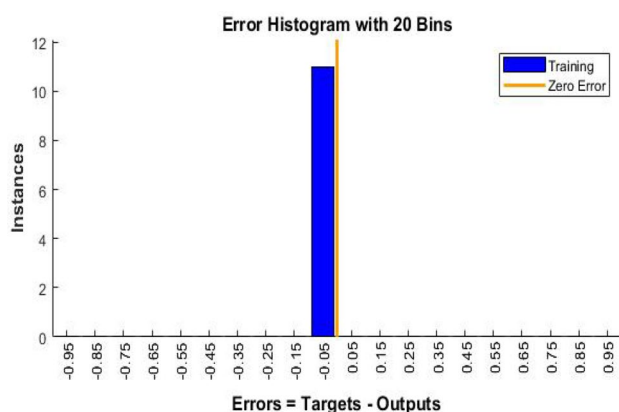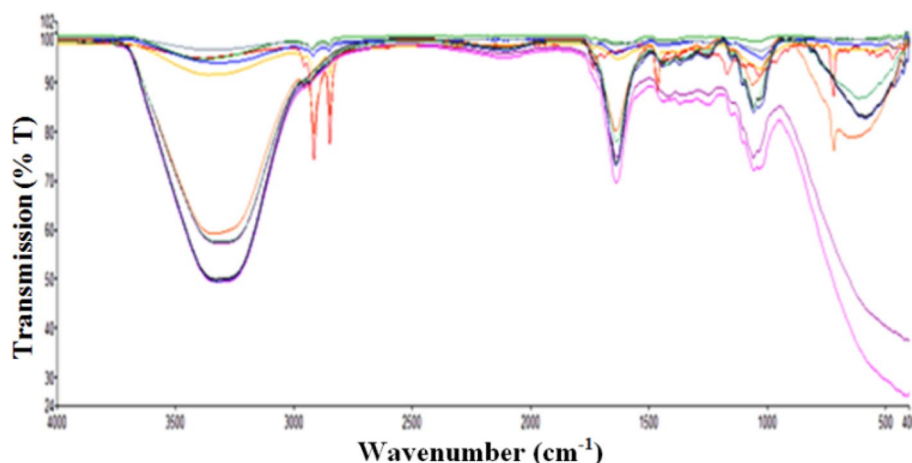**Fig. 18** Comparative FTIR analysis of apple samples

Fig. 19 Plot of error histogram

imaging-based sensor captures both the external and internal features of the samples, hence, improves the predicting capability and accuracy of FDPM. In Table 3, the parameters for data normalization of neural network is shown that shows the epoch, batch size, k-fold cross validation, dataset, type of image, and accuracy.

5 Conclusions

In this paper, a three-level validation process (RGB-Thermal, FTIR, and destructive) has been adopted to identify defects in apple samples. In the FTIR, healthy and defected apple samples are compared, and missing functional groups are identified. This gap helps to distinguish between healthy and defected apples. A deep learning-based prediction model is developed. The model utilizes features information received from RGB and thermal images of the apple samples. Among available classifier models, the Naïve Bayes classifier detects and recognizes the defects in the apple with an accuracy of 97.6% for thermal IR imaging information and shows 59% of accuracy for true color (RGB) image information of the same sample. It has been observed from the thermogram color pallet of the fruit that the healthy tissues show uniform heat distribution whereas unhealthy tissues show non-uniform heat distribution. To validate the prediction made by the deep learning-based classifier model, FTIR analysis and destructive operation is done under the
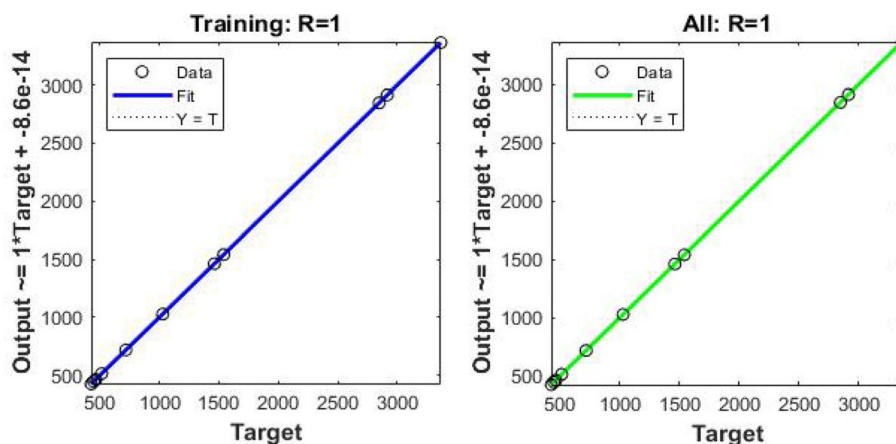
Fig. 20 Plot of regression curve

Table 2 Performance comparision of classification methods for fruit defect prediction

Sample	Classifier	Prediction speed (obs/s)	Training time (s)	Observation	Predictors	Accuracy (%)
IR Imaging (10-Fold Cross-Validation)	Naïve Bayes	360	3.66	45	8	97.6
	Logistic Regression	540	11.97	45	8	93.3
	Fine Gaussian SVM	740	2.3	45	8	91.1
	Cubic KNN	530	1.6	45	8	91.1
True colour (10-Fold cross-validation)	Logistic Regression	610	1.2	39	8	69.2
	Naïve Bayes	440	1.8	39	8	59
	Fine Gaussian SVM	940	1.03	39	8	71.8
	Cubic KNN	720	0.98	39	8	79.5

Table 3 Parameters for data normalization

Epoch	Batch Size	K fold cross validation	Dataset	Image	Accuracy (%)
100	15	15	500	Thermal	97.6
100	15	15	800	RGB	59

second and third level of the validation process FDPM. The performance comparison of the prediction model is presented in Table 2. From Table 2, it is concluded that the proposed FDPM classifier shows good performance. The proposed FDPM reduces the amount of fruit wastage during the testing and validation process. This approach will certainly reduce the human efforts and involvements for testing and validation which involves a rigorous chemical and biochemical process to achieve the same goal. The FDPM will also be helpful in maintaining a chemical-free environment and to make human beings healthy.

The proposed FDPM can further be extended to predict the ripeness percentage of the fruits, internal disorder due to chemical effects, and to check the nutrients deficiency of fruits.

References

1. Thangavelns, K., Dhivya, K.: Determination of curcumin, starch and moisture content in turmeric by Fourier transform near infrared spectroscopy (FT-NIR). Eng. Agric. Environ. Food **12**, 264–269 (2019)
2. Mohd, M.R.S., Herman, S.H., Shariff, Z.: Application of discrete wavelet transform in thermal infrared image processing. In: *2016 IEEE Conference on Systems, Process and Control (ICSPC), Bandar Hilir*, 2016, pp. 186–191. https://doi.org/10.1109/SPC.2016.7920727.
3. Mulaveesala, R., Ghali, V.S., Arora, V.: Applications of non-stationary thermal wave imaging methods for characterisation of fibre-reinforced plastic materials. Electron. Lett. **49**(2), 118–119 (2013)
4. Liu, Q., Hong, X., Zou, B., Chen, J., Chen, Z., Zhao, G.: Hierarchical contour closure-based holistic salient object detection. IEEE Trans. Image Process. **26**(9), 4537–4552 (2017). https://doi.org/10.1109/TIP.2017.2703081
5. Meng, F., Li, H., Wu, Q., Luo, B., Ngan, K.N.: Weakly supervised part proposal segmentation from multiple images. IEEE Trans. Image Process. **26**(8), 4019–4031 (2017). https://doi.org/10.1109/TIP.2017.2708839
6. Raghavendra, A., Rao, M.: A survey on internal defect detection in fruits by non-intrusive methods. Int. J. Latest Trends Eng. Technol. **6**(3), 343–348 (2016)
7. Wang, F., Pan, X.: Image segmentation for somatic cell of milk based on niching particle swarm optimization Otsu. Eng. Agric. Environ. Food **12**, 141–149 (2019)
8. Leena, N., Saju, K.K.: Classification of macronutrient deficiencies in maize plants using optimized multi class support vector machines. Eng. Agric. Environ. Food **12**, 126–139 (2019)
9. Serrato, K.L.R., Estrada, J.A.S., Gonzalez, M.T.R.: Automatic pest detection on bean and potato crops by applying neural classifiers. Eng. Agric. Environ. Food **11**, 245–255 (2018)
10. Sa, J., Sun, X., Zhang, T., Li, H., Zeng, H.: Improved Otsu segmentation based on Sobel operator. In: 2016 3rd Intl. Conf. on Systems and Informatics (ICSAI), Shanghai, pp. 886–890 (2016).
11. Khan, M.B., Nisar, H., Aun, N.C., Lo, P.K.: Iterative region-based Otsu thresholding of bright-field microscopic images of activated sludge. In: 2016 IEEE EMBS Conference on Biomedical Engineering and Sciences (IECBES), Kuala Lumpur, pp. 533–538 (2016). https://doi.org/10.1109/IECBES.2016.7843507.
12. Wang, Q., Hu, S., Wang, J., Ren, K.: Secure surfing: privacy-preserving speeded-up robust feature extractor. In: 2016 IEEE 36th International Conference on Distributed Computing Systems (ICDCS), Nara, pp. 700–710 (2016). https://doi.org/10.1109/ICDCS.2016.84.
13. Abedin, M.Z., Dhar, P., Deb, K.: Traffic sign recognition using SURF: speeded up robust feature descriptor and artificial neural network classifier. In: 2016 9th International Conference on

Electrical and Computer Engineering (ICECE), Dhaka, pp. 198–201 (2016). https://doi.org/10.1109/ICECE.2016.7853890.

14. Verma, N.K., Sharma, T., Sevakula, R.K., Salour, A.: Vision based object counting using speeded up Robust features for inventory control. In: 2016 International Conference on Computational Science and Computational Intelligence (CSCI), Las Vegas, NV, pp. 709–714 (2016). https://doi.org/10.1109/CSCI.2016.0139.

15. Melendez, J., Girones, X., Puig, D.: Supervised texture segmentation through a multi-level pixel-based classifier based on specifically designed filters. In: 2011 18th IEEE International Conference on Image Processing, Brussels, pp. 2869–2872 (2011). https://doi.org/10.1109/ICIP.2011.6116147.

16. Zhang, K., Xu, Z., Dong, S., Con, C., Wu, Q.: Identification of peach leaf disease infected by *Xanthomonas campestris* with deep learning. Eng. Agric. Environ. Food **12**(4), 388–396 (2019)

17. Wdowiak, M., Slodkowska, J., Markiewicz, T.: Cell segmentation in desmoglein-3 stained specimen microscopic images using GVF and watershed algorithm. In: 2016 17th International Conference Computational Problems of Electrical Engineering (CPEE), Sandomierz, pp. 1-3 (2016). https://doi.org/10.1109/CPEE.2016.7738760

18. Mohana Rao, K.N.R., Dempster, A.G.: Modification on distance transform to avoid over-segmentation and under-segmentation. In: Intl. Symposium on VIPromCom Video/Image Processing and Multimedia Communications, Zadar, Croatia, pp. 295–301 (2002). https://doi.org/10.1109/VIPROM.2002.1026672.

19. Duarte, A., Carrão, L., Espanha, M., Viana, T., Freitas, D., Bártolo, P., Faria, P., Almeida, H.A.: Segmentation algorithms for thermal images. Procedia Technol. **16**, 1560–1569 (2014)

20. Font-Aragones, X., Faundez-Zanuy, M., Mekyska, J.: Thermal hand image segmentation for biometric recognition. IEEE Aerosp. Electron. Syst. Mag. **28**(6), 4–14 (2013). https://doi.org/10.1109/MAES.2013.6533739

21. Chen, Y., Chen, W., Ni, H.: Image segmentation in thermal images. In: 2016 IEEE International Conference on Industrial Technology (ICIT), Taipei, pp. 1507–1512 (2016). https://doi.org/10.1109/ICIT.2016.7474983.

22. Shaikh,S., Gite, H., Manza, R.R., Kale, K.V., Akhter, N.: Segmentation of thermal images using thresholding-based methods for detection of malignant tumours. In: Intl. Symposium on Intelligent Systems Technologies and Applications, Advances in Intelligent Systems and Computing (AISC), vol. 530, pp. 131–146 (2016).

23. Jaffery, Z.A., Dubey, A.K.: Design of early fault detection technique for electrical assets using infrared thermograms. Int. J. Electric. Power Energy Syst. **63**, 753–759 (2014)

24. Jaffery, Z.A., Dubey, A.K., Irshad, Haque, A.: Scheme for predictive fault diagnosis in photo-voltaic modules using thermal imaging. Infrared Phys. Technol. **83**, 182–187 (2017)

25. Spahn, J.G., Nuguru, K.: Grayscale thermographic imaging. US patent, US 20160213304 A1 (2016).

26. Usamentiaga, R., Venegas, P., Guerediaga, J., Vega, L., Molleda, J., Bulnes, F.G.: Infrared thermography for temperature measurement and non-destructive testing. Sensors **14**(7), 12305–12348 (2014)

27. Santhi, V.: Recent advances in applied thermal imaging for industrial applications. IGI Global (2017). https://doi.org/10.4018/978-1-5225-2423-6

28. http://www.giangrandi.ch/optics/blackbody/blackbody.shtml. Accessed 19 Aug 2017

29. http://www.physicscentral.com/explore/action/infraredlight.cfm. Accessed 19 Aug 2017

30. https://physics.stackexchange.com/questions/116302/how-is-temperature-related-to-color. Accessed 19 Aug 2017

31. http://www.iar.unicamp.br/lab/luz/ld/Cor/color_vision.pdf. Accessed 19 Aug 2017

32. Jeroen, et al.: Light penetration properties of NIR radiation in fruit with respect to non-destructive quality assessment. Postharv. Biol. Technol. **18**(2), 121–132 (2000)

33. Davidhazy, A.: Infrared photography. https://people.rit.edu/andpph/text-infraredbasics.html. Accessed 19 Aug 2017

34. https://www.simac.com/en/type-oplossingen/thermal-vision-inspection. Accessed 19 Aug 2017

35. http://www6.dict.cc/wp_examples.php?lp_id=1&lang=en&s=human%20eye. Accessed 19 Aug 2017

36. Prabhakar, C.J., Mohana, S.H.: Computer vision based technique for surface defect detection of apples. In: Srivastava, R., Singh, S.K., Shukla, K.K. (eds.) Research Developments in Computer Vision and Image Processing: Methodologies and Applications, pp. 111–121. Idea Group, New York (2014)

37. Using Regions of Interest as Masks. http://www.xinapse.com/Manual/roi_mask.html. Accessed 19 Aug 2017

38. Kim, H.S.: FPGA-based of thermogram enhancement algorithm for non-destructive thermal characterization. IJE Trans. A Basics **31**(10), 1675–1681 (2018)

39. Shavandi, M., Afrakoti, I.E.P.: Face recognition in thermal images based on sparse classifier. IJE Trans. A Basics **32**(1), 78–84 (2019)

40. Mysteries of Neural Networks. https://towardsdatascience.com/gentle-dive-into-math-behind-convolutional-neural-networks-79a07dd44cf9. Accessed 27 Jan 2020.

41. Hahn, F.: Actual pathogen detection: sensors and algorithms—a review. Algorithms **2**, 301–338 (2009)

42. Pan, J., et al.: Image segmentation based on 2D OTSU and simplified swarm optimization. In: 2016 International Conference on Machine Learning and Cybernetics (ICMLC), Jeju, pp. 1026–1030 (2016). https://doi.org/10.1109/ICMLC.2016.7873020.

43. Stefan, J.: Über die Beziehung zwischen der Wärmestrahlung und der Temperatur [On the relationship between heat radiation and temperature] (PDF), Sitzungsberichte der mathematisch-naturwissenschaftlichen Classe der kaiserlichen Akademie der Wissenschaften (in German). Vienna **79**, 391–428 (1879)

44. Hassanpour, H., Yousefian, H.: An improved pixon-based approach for image segmentation. IJE Trans. A Basics **24**(1), 25–35 (2011)

45. Yogesh, Dubey, A.K., Ratan, R., Rocha, R.: Computer vision based analysis and detection of defects in fruits causes due to nutrients deficiency. Cluster Comput. (2019). https://doi.org/10.1007/s10586-019-03029-6

Yogesh received the B.Tech. degree in Electronics & Communication Engineering from M.A.C.E.T. Patna, Bihar, India in 2007 and M.Tech. degree in Electronics & Communication Engineering from Amity University, Noida, Uttar Pradesh, India in 2013. Presently, he is a Ph.D. Research Scholar in the Department of Electronics & Communication Engineering, Amity School of Engineering and Technology, Amity University Uttar Pradesh, Noida, Uttar Pradesh, India and working as an Assistant Professor in the Department of Electronics & Communication

Engineering, Amity School of Engineering and Technology, Amity University Uttar Pradesh, Noida, Uttar Pradesh, India. He has filed 20 patents and published 30 research papers in various international conferences and journals of repute. His current research interests include digital image processing and computer vision.

Ashwani Kumar Dubey received the M.Tech. degree in Instrumentation and Control Engineering from Maharshi Dayanand University, Rohtak, Haryana, India, in 2007, and a Ph.D. degree from the Department Electrical Engineering, Faculty of Engineering and Technology, Jamia Millia Islamia (A Central Govt. University), New Delhi, India, in 2014. Currently, he is an Associate Professor in the Department of Electronics and Communication Engineering, Amity School of Engineering and Technology, Amity University Uttar Pradesh, Noida, Uttar Pradesh, India. He has published more than 60 research papers in SCI/Scopus indexed Journals and IEEE Conferences. He has filed 20 patents. He is the Organizing Chair of IEEE sponsored International Conference on Signal Processing and Integrated Networks (SPIN) since 2019. His research interests includes computer vision, digital image processing, NDT, sensors, and wireless sensor networks.

Rajeev Ratan Arora received the M.Tech. Degree in Instrumentation & Control Engineering from Maharishi Dayanand University, Rohtak, Haryana in 2007 and a Ph.D. degree from the Department of Electronics & Communication Engineering, Thapar University, Patiala, Punjab in 2014. He is a lifetime member of Indian Society of Technical Education (ISTE), New Delhi, India and Associate Member of Institution of Engineers (IE), India. He has published more than 30 research papers in IEEE Conferences and SCI/Scopus indexed Journals. His research interests are Digital Signal Processing, FPGA Design, Embedded Systems, Image Processing and Biomedical Instrumentation.

Ashish Mathur received the Ph.D degree from NIBEC, University of Ulster, Jordanstown campus, Belfast, U.K. in 2011, M.Tech (Nanotechnology) from Amity Institute of Nanotechnology, Amity University, Noida, India in 2007, M.Sc (Electronics) from CSJM University, Kanpur, India in 2005, and B.Sc. (Electronics) from CSJM University, Kanpur, India in 2003. Currently he is working as an Associate Professor Department of Physics, School of Engineering, UPES University, Bidholi Campus, Dehradoon, India. He worked as an Assistant Professor with Amity Institute of Nano Technology, Amity University Uttar Pradesh, Noida, Uttar Pradesh, India. He also worked as Research Associate at NIBEC, University of Ulster, Jordanstown campus, Belfast, U.K, from July 2010-Dec 2012. His research interest includes Microfluidics, Sensors, Carbon Nano- structures, MEMS and NEMS.